

Characteristics of Arctic polar stratospheric clouds in the winter of 1996/1997 inferred from ILAS measurements

N. Saitoh,¹ S. Hayashida,¹ Y. Sasano,² and L. L. Pan³

Received 5 March 2001; revised 12 October 2001; accepted 6 November 2001; published 19 September 2002.

[1] The Improved Limb Atmospheric Spectrometer (ILAS) captured many polar stratospheric cloud (PSC) events in the Northern Hemisphere during the winter and early spring of 1997. Simultaneous measurements of nitric acid and aerosols by ILAS made it possible to infer PSC composition. The aerosol extinction coefficient and nitric acid data were compared with the theoretically predicted values for supercooled ternary solution (STS), nitric acid dihydrate (NAD), and nitric acid trihydrate (NAT) at thermodynamic equilibrium to classify PSC types. The observations showed that in 1997, both nitric-acid-containing solid and liquid PSCs formed over the Arctic during winter and early spring, until mid-March. The STS PSCs were observed early in the PSC season, in mid-January. Most of the PSCs observed late in the PSC season had features of nitric-acid-containing hydrates. An intensive analysis of the temperature histories suggested that most of the STS events observed in January had experienced the thermal conditions necessary for the formation of liquid PSCs. The nitric-acid-containing hydrates observed in March seemed not to have been influenced by any mountain-induced lee waves. The process of nitric-acid-containing hydrate formation based on synoptic scale temperature change is discussed. *INDEX TERMS:* 0305

Atmospheric Composition and Structure: Aerosols and particles (0345, 4801); 0340 Atmospheric Composition and Structure: Middle atmosphere—composition and chemistry; 1640 Global Change: Remote sensing; 1610 Global Change: Atmosphere (0315, 0325)

Citation: Saitoh, N., S. Hayashida, Y. Sasano, and L. L. Pan, Characteristics of Arctic polar stratospheric clouds in the winter of 1996/1997 inferred from ILAS measurements, *J. Geophys. Res.*, 107(D24), 8205, doi:10.1029/2001JD000595, 2002.

1. Introduction

[2] Polar stratospheric clouds (PSCs) cause large amounts of ozone depletion in the lower stratosphere in both pole regions, by providing a situation that allows heterogeneous reactions that convert inactive reservoir chlorine into active chlorine [Solomon, 1999]. PSCs also remove nitric acid from the gas phase irreversibly, which prevents deactivation of active chlorine. The phase and chemical composition of PSCs are important factors in accurately estimating the amount of ozone loss and revealing the mechanism of ozone destruction during polar winter in more detail. Ravishankara and Hanson [1996] and Borrmann *et al.* [1997] suggested that liquid droplets convert inactive chlorine to an active form more efficiently than do frozen particles. In addition to their function in heterogeneous reactions, solid particles play an important role in redistribution of NO_y and water vapor via sedimentation. The temperatures over the Arctic seldom fall below the temperature at which ice particles are formed; therefore, solid

particles containing nitric acid (nitric acid hydrates) are thought to be a predominant factor in the large-scale denitrification observed in the Arctic [e.g., Waibel *et al.*, 1999; Fahey *et al.*, 2001; Tabazadeh *et al.*, 2001].

[3] Lidar measurements are an effective technique for inferring the composition of PSCs directly. The scattering ratio and depolarization observed with lidar make it possible to categorize the PSC types as type 1a (large depolarization and small scattering ratio), type 1b (small depolarization and large scattering ratio), or type 2 (large depolarization and large scattering ratio) [Browell *et al.*, 1990]. Carslaw *et al.* [1994] showed that the observed type 1b PSCs would be supercooled ternary solutions (STS), based on a thermodynamic model, and measurements of the infrared spectra of PSCs support the existence of STS [Toon and Tolbert, 1995]. Backscatter sonde measurements show substantial growth of liquid droplets at several degrees below T_{NAT}, suggesting the existence of STS [Larsen *et al.*, 1996]. While both the composition and formation mechanism of liquid type 1b PSCs are clear to some extent, those of solid type 1a PSCs remain unclear [Tolbert, 1996]. Type 1a PSCs could be nitric acid hydrates, such as nitric acid trihydrate (NAT), nitric acid dihydrate (NAD), or nitric acid pentahydrate (NAP) [Hanson and Mauersberger, 1988; Worsnop *et al.*, 1993; Marti and Mauersberger, 1994].

[4] Tolbert [1994, 1996] reviewed the formation mechanisms of PSCs over a polar winter. The solid particles that

¹Faculty of Science, Nara Women's University, Nara, Japan.

²National Institute for Environmental Studies, Tsukuba, Ibaraki, Japan.

³Atmospheric Chemistry Division, National Center for Atmospheric Research, Boulder, Colorado, USA.

are often observed over the Arctic [e.g., *Browell et al.*, 1990] cannot simply be interpreted as nucleation on ice nuclei, because the synoptic temperatures seldom fall below the ice frost point over the Arctic. Recently, many studies have examined the effect of mountain-induced lee waves on solid particle formation [*Tsias et al.*, 1997; *Carshaw et al.*, 1998, 1999; *Riviere et al.*, 2000]. The formation mechanisms of PSCs are so complex that the thermal conditions the particles have experienced should also be examined closely, in addition to the temperature where they are observed. Many studies of synoptic temperature histories have been carried out using in situ [*Larsen et al.*, 1996, 1997] and satellite [*Santee et al.*, 1998; *Riviere et al.*, 2000] measurements.

[5] Some studies suggest that satellite measurements have good potential for investigating the chemical composition and physical state of PSCs. *Massie et al.* [1997] used the data obtained with the Microwave Limb Sounder (MLS), the Cryogenic Limb Array Etalon Spectrometer (CLAES), and the Improved Stratospheric and Mesospheric Sounder (ISAMS) on board the Upper Atmosphere Research Satellite (UARS) to study the formation of PSCs over Scandinavia. *Hervig et al.* [1997] compared the Halogen Occultation Experiment (HALOE) aerosol data with the calculated volume of several types of PSCs. *Santee et al.* [1998] investigated the composition of PSCs over the Antarctic using nitric acid data measured with the MLS, and *Santee et al.* [2000] combined the MLS nitric acid data with the aerosol extinction coefficient data obtained from the Polar Ozone and Aerosol Measurement (POAM) II.

[6] The Improved Limb Atmospheric Spectrometer (ILAS) on board the Advanced Earth Observing Satellite (ADEOS) is a solar occultation sensor [*Sasano et al.*, 1999] with two spectrometers: a 44-channel infrared (IR) spectrometer operating from 6.21 to 11.76 microns, and a 1024-channel near-visible spectrometer operating at wavelengths from 753 to 784 nm [*Suzuki et al.*, 1995; *Nakajima et al.*, 2002]. ILAS was designed to observe the profiles of minor stratospheric species, such as ozone, nitric acid, and water vapor, and that of the stratospheric aerosol extinction coefficient at 1-km height intervals [*Yokota et al.*, 2002]. Due to the Sun-synchronous polar orbit of ADEOS, ILAS observed 14 circumpolar points in each hemisphere every day at high latitudes (57.1–72.7°N and 64.3–88.2°S). ILAS started regular operation in November 1996 and continued until June 1997. In inferring PSC composition, simultaneous measurements of aerosol extinction and nitric acid for the same air mass are desirable. *Hayashida et al.* [2000a] reported that the ILAS captured more than 60 PSC profiles in the Northern Hemisphere during the winter and early spring of 1997, and showed their temporal and spatial

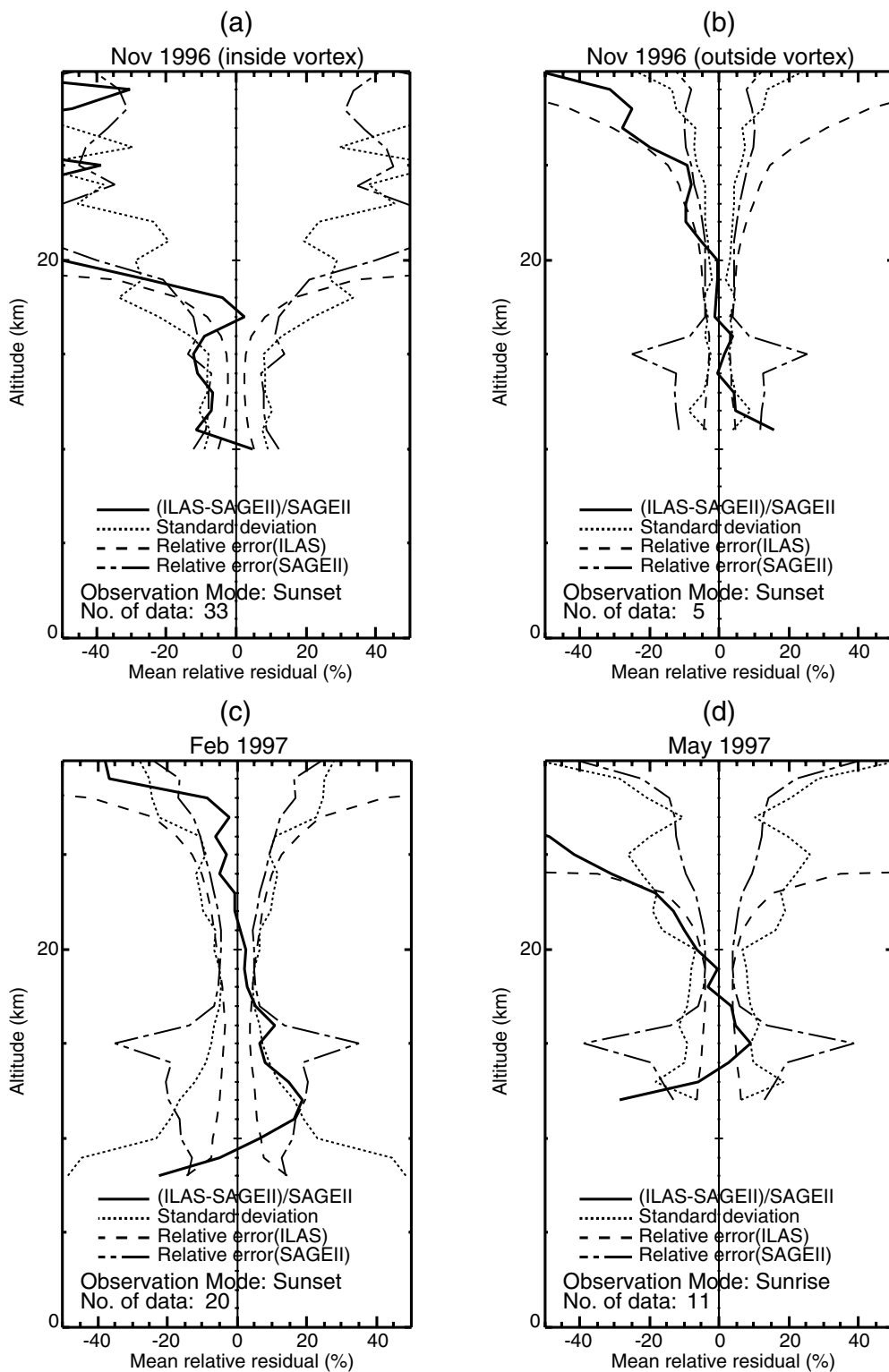
distributions. The aim of this study was to infer the composition of the PSC particles observed from ILAS aerosol and nitric acid data. The synoptic temperature histories of air masses containing the observed PSCs are also examined to compare the results with PSC formation theory.

[7] The latest retrieval (version 5.20) of ILAS data was used in this study. The version 3.10 and 5.20 ILAS nitric acid data were validated by *Koike et al.* [2000] and *Irie et al.* [2002], respectively, demonstrating the reliability of the data. The version 5.20 ILAS water vapor data was validated by *Kanzawa et al.* [2002]. The inversion algorithm and validity of version 4.20 of the ILAS aerosol extinction data have been described by *Hayashida et al.* [2000a]. Details of the version 5.20 algorithm were described by *Yokota et al.* [2002]. Here, we briefly present the differences between version the 5.20 and version 4.20 data. Figure 1 is comparable with the Figure 3 of *Hayashida et al.* [2000a], which compared Stratospheric Aerosol and Gas Experiment (SAGE) II version 6.0 data and ILAS version 5.20 data. For comparison, we selected pairs of coincident measurements with ILAS and SAGE II when the distance between the two measurement locations was within 300 km and the measurement time difference was less than 120 min. As a result, 38 profiles in November 1996 and 20 profiles in February 1997 were selected over the Southern Hemisphere, and 11 profiles in May 1997 over the Northern Hemisphere. The November data were separated into two groups, containing profiles inside (33 profiles) or outside (5 profiles) the polar vortex. Each panel depicts the mean fractional difference between the ILAS and SAGE II data (solid line), the root mean square of the fractional difference (dotted line), and the ILAS (dashed line) and SAGE II (dashed and dotted line) measurement errors. The mean fractional differences are within the uncertainties of the ILAS and SAGE II measurement errors, and are in the range of 10–20% where the extinction values are larger than $1.0 \times 10^{-5} \text{ km}^{-1}$, demonstrating the validity of the ILAS version 5.20 aerosol data for scientific use.

2. PSC Identification

[8] Our approach to identifying PSCs is similar to those of *Poole and Pitts* [1994] and *Fromm et al.* [1997]. In these studies, threshold levels were determined from the background aerosol levels, and then events with an extinction exceeding the threshold levels were regarded as PSC events. In the method that we adopted by *Hayashida et al.* [2000a], all the extinction data inside the polar vortex were averaged for each altitude interval and for each 10-day period where the collocated temperature was above 200 K, and the mean was defined as the background aerosol level of each period.

Figure 1. (opposite) Comparison of the extinction coefficient at 780 nm using ILAS version 5.20 and SAGE II version 6.0. For comparison, we selected pairs of coincident ILAS and SAGE II measurements when the distance between the two measurement locations was within 300 km and the measurement time difference was less than 120 min. The 38 coincident profiles observed in November 1996 were divided into two groups depending on whether they were inside or outside the polar vortex. From the left, comparisons of (a) 33 profiles over the Southern Hemisphere in November 1996 inside the vortex, (b) 5 profiles outside the vortex in the same month, (c) 20 profiles over the Southern Hemisphere in February 1997, and (d) 11 profiles over the Northern Hemisphere in May. Each panel depicts the mean fractional difference between the ILAS and SAGE II data (solid line), the root-mean-square of the fractional difference (dotted line), the ILAS measurement error (dashed line), and the SAGE II measurement error (dashed and dotted line). The SAGE II extinction coefficients at 525 nm and 1020 nm were converted to 780 nm by linearly interpolating the logarithms of the extinction coefficients.



The mean plus five standard deviations was adopted as the threshold value after close examination; events whose extinction value exceeded the threshold value for the same period, and whose relative error did not exceed 100%, were identified as PSCs (“5sigma-selected” events) (about the estimation of total error, see the Appendix of *Hayashida et al.* [2000a]). In the analysis of *Hayashida et al.* [2000a], insufficient data on background aerosols ($T > 200$ K), especially during the cold period in mid-January, reduced the statistical reliability of the threshold values for the period [see *Hayashida et al.*, 2000a, Figure 5].

[9] Our improved approach considered the data obtained for 5 days before and after each 10-day period in addition to the data during the period. This approach produced more realistic thresholds. Nevertheless, appropriate threshold values for mid-January upper than 26 km could not be determined. However, this did not affect our analysis significantly, because PSCs were rarely observed at such high altitudes. We identified about 250 events using this improved approach; it did not alter the trend of PSC distribution shown by *Hayashida et al.* [2000a]. Although *Hayashida et al.* [2000a] had adopted the NAT formation temperature, T_{NAT} , as one possible reference to validate PSC identification, we also investigated all PSC events exceeding the threshold, including those at collocated temperatures higher than T_{NAT} .

3. Comparison of the ILAS Data With Theoretical Predictions

[10] Comparison of the observed aerosol mass or nitric acid data with the values predicted from thermodynamic theory for various PSC types allows us to infer the chemical composition of observed particles [e.g., *Massie et al.*, 1997; *Santee et al.*, 1998, 2000]. As the amounts of nitric acid and water vapor in the atmosphere are closely concerned with PSC composition, it is important to estimate those amounts properly in inferring PSC composition.

[11] The ILAS observed the vertical profiles of nitric acid and water vapor, and the aerosol extinction coefficient simultaneously. Using these observed data to calculate the theoretically predicted values for various PSC types, we can infer PSC composition more precisely than using climatological values, as done in earlier works. In the following, we describe how we determine the total amounts of nitric acid, water vapor, and sulfuric acid properly, based on the ILAS collocated gas and aerosol data. The total amount is the equivalent mixing ratio of gas and condensed phase combined. In this study, the ILAS data were compared with theoretical values of particle volume and gaseous nitric acid, assuming the existence of STS, NAD, and NAT.

3.1. Total Amounts of Nitric Acid and Water Vapor in the Background Stratosphere

[12] The total amounts of nitric acid and water vapor in the atmosphere required in theoretical calculations were estimated from ILAS nitric acid and water vapor data. All nitric acid and water vapor data inside the polar vortex were averaged for each altitude level and for each 10-day period in the region where the collocated temperature exceeded 200 K, and the average values were taken as the total background amounts of nitric acid and water vapor, respec-

tively, for each period. Data with a relative error exceeding 100% were excluded from the calculation. For example, the amounts of nitric acid and water vapor at 20 km near 65°N in mid-January were estimated from the observations as 11.4 ppbv and 5.2 ppmv.

3.2. Total Amount of Sulfate in the Background Stratosphere

[13] The weight percentage of sulfate in stratospheric particles depends only on temperature and humidity [*Steele and Hamill*, 1981]. The total amount of sulfate in the atmosphere can be derived from the ILAS extinction profiles. The analytic expression of *Carslaw et al.* [1995] gives the particle volume of $\text{H}_2\text{SO}_4/\text{H}_2\text{O}$ binary aerosol in warmer conditions.

[14] We calculated the particle volumes in the background condition for various quantities of sulfate, applying the values of water vapor estimated from the ILAS data. The particle volume was converted into extinction coefficients at 780 nm for comparison with ILAS extinction data. The conversion factors from volume to extinction were derived by applying Mie scattering theory with the refractive indices of $\text{H}_2\text{SO}_4/\text{H}_2\text{O}$ binary solution ($n = 1.449$, $T = 223$ K, $0.781 \mu\text{m}$) [*Russell et al.*, 1996]. Two different size distributions for the background conditions were assumed in the calculations. One was that measured with the optical particle counter (OPC) at midlatitudes [*Hofmann and Rosen*, 1983], and the other was that from the OPC data obtained over Esrange/Kiruna (67.88°N, 21.06°E) in February 1997 during the ILAS validation campaign [*Deshler et al.*, 2000], when no PSCs were detected. Comparison showed that the conversion factors for the different size distributions were not significantly different. The conversion factors were also determined based on the Ångström parameter derived from SAGE II aerosol extinction coefficient data [*Hayashida et al.*, 2000b]. They were consistent with the above two conversion factors quantitatively, which confirms the validity of the conversion factors used here. For example, the estimated amount of sulfate was 0.25 ppbv at 20 km near 65°N in mid-January. Details of the scheme to estimate total sulfate were described by *Hayashida et al.* [2000b].

3.3. Calculation of Nitric Acid and Particle Volume Based on Thermodynamic Theory

[15] The theoretical particle volume for the formation of STS and the amount of remaining gaseous nitric acid in the atmosphere were calculated by applying *Carslaw et al.*'s [1995] analytic expression. The total amounts of nitric acid, water vapor, and sulfate were derived as described above. The vapor pressures of nitric acid in equilibrium over NAD and NAT were calculated, based on *Worsnop et al.* [1993] and *Hanson and Mauersberger* [1988], respectively. The expected particle volumes for NAD and NAT were calculated using a mass density of 1.62 g/cm^3 for NAT [*Hofmann and Deshler*, 1991].

[16] The theoretical particle volumes have to be converted into 780 nm extinction coefficients for comparison with the ILAS aerosol extinction data. The conversion factors for PSC cases were derived using the temperature-dependent refractive indices of STS [*Luo et al.*, 1996], NAD, and NAT [*Toon et al.*, 1994]. The bimodal size distribution fitted to OPC data measured over Andoya

(69.3°N, 16.0°E) in January 1997 [Deshler *et al.*, 2000] was adopted in this study. Comparison of the conversion factors for several different particle size distributions for PSCs [Dye *et al.*, 1992] suggested that the size distributions of PSCs are more uncertain than those of background aerosols. This should be considered when inferring PSC composition.

3.4. Comparison of the ILAS Data With Theoretical Predictions

3.4.1. Mid-January

[17] Figure 2 shows scatterplots of UKMO temperature versus the ILAS extinction coefficient (left column), and UKMO temperature versus the ILAS nitric acid value (right column), at 20–23 km in mid-January. Each panel represents a 1-km altitude level. Solid circles represent the data identified as PSCs. Error bars for the ILAS data are shown in the figure, although not all are distinguishable. The theoretical curves for STS (red lines), NAD (green line), and NAT (blue line) are shown in the figure. As for NAD and NAT, their formation curves are derived with the mass-to-extinction conversion factor for PSC size distribution function. The PSC conversion factor for growth curve of ternary solution should be applied only at cold temperatures where STS droplets are expected to form, while the background conversion factor should be used at warm temperatures. In Figure 2, STS formation curves are indicated with the thick solid red lines with the proper conversion factors depending on temperatures, though the thin dotted red lines are also shown for reference. The low extinction values at warmer temperatures are consistent with the theoretical curve expected for background (binary) aerosols. In the figure, the red circles indicate events whose extinction and nitric acid values are closest to theoretical STS values among three types. Figures 2a and 2b show that the enhancement of the volume corresponds to the decrease in the ambient nitric acid, suggesting the uptake of nitric acid into particles as STS forms.

[18] In Figure 2, the data numbered 1 to 4 are from the same profile, observed on 19 January (65.8°N, 21.6°E, Figure 3a), and those numbered 5 to 8 are from 20 January (65.9°N, 28.9°E, Figure 3b). Figure 3 shows the vertical profiles of the extinction coefficient (E), nitric acid (N), and the collocated UKMO temperature (T) on these two days. The 10-day averaged background profile of nitric acid for mid-January is also shown in the figure (dashed line). The black and gray circles represent data identified as PSCs. The black circles indicate the data that correspond to the STS formation curve. Figure 3 shows that STS-like PSCs were observed over a wide vertical range on these days. Comparison of the ILAS nitric acid profile with the background profile illustrates that nitric acid decreased significantly in the region where STS PSCs were observed.

[19] Besides the characteristic agreement with thermodynamic model prediction shown above, two other independent analyses support the presence of STS in these observed PSC events. One is given by the spectral analyses of ILAS extinction data. The aerosol extinction coefficients derived from the ILAS visible and four infrared window channels (at 7.12, 8.27, 10.6, and 11.8 μm) show that the spectral features for these events are STS-like (S. Oshchepkov, private communication, 2001). The other is from coincident ground based lidar measurements. Both of GKSS Raman-

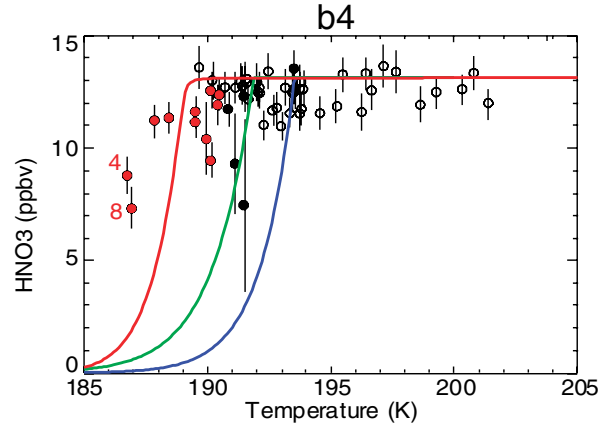
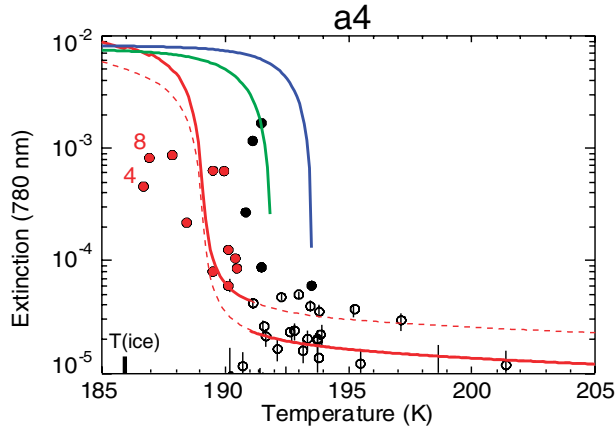
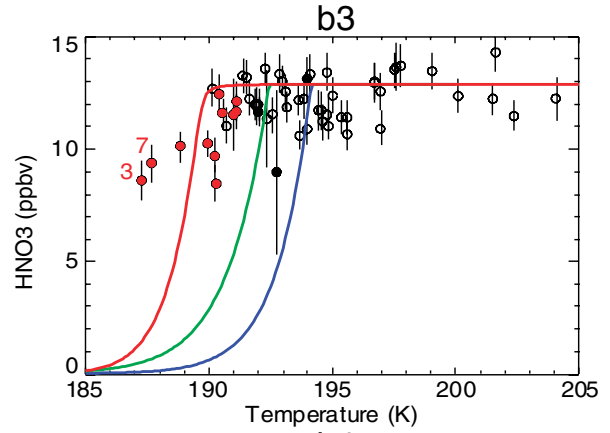
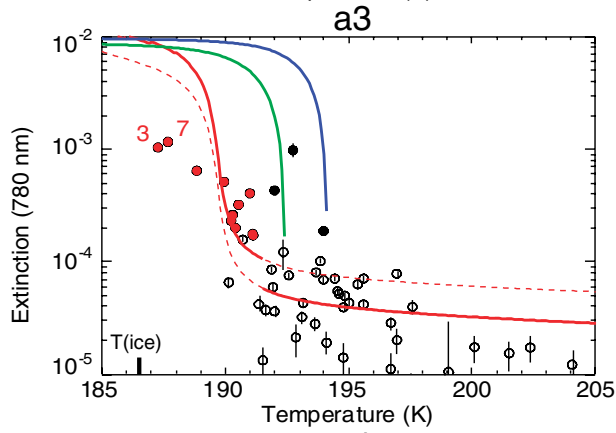
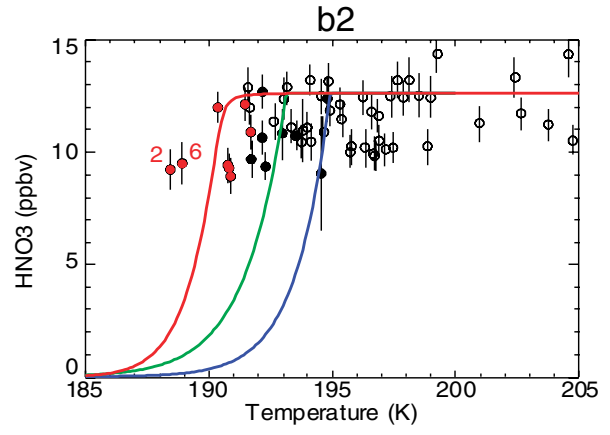
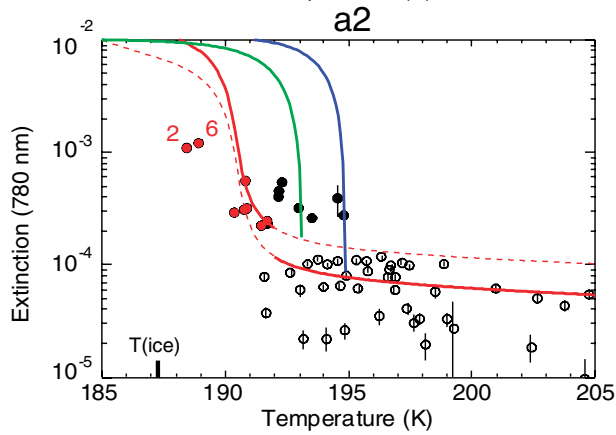
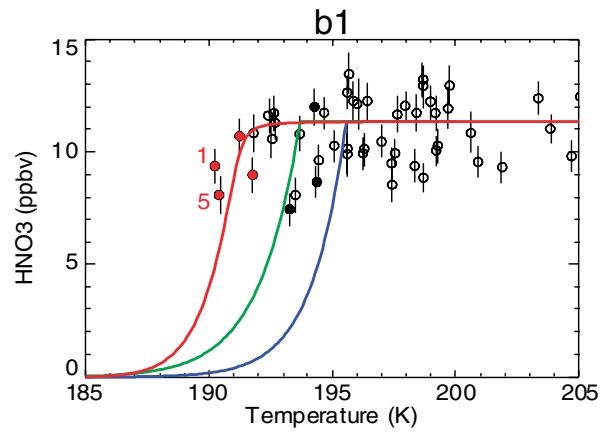
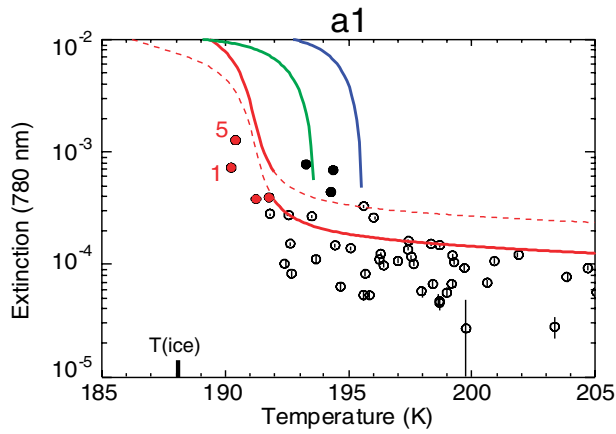
lidar and a Mie-lidar of Bonn University observed type 1b events on 19 and 20 January continuously at 19.0–24.5 km over Esrange/Kiruna (67.88°N, 21.06°E) [Mehrtens and Reichardt, 1997; Dörnbrack *et al.*, 2001]. These Lidar observations were made in the vicinity of ILAS observations shown in Figure 3 (about 270 km and 450 km away from the profiles in Figures 3a and 3b, respectively), providing good validation to our analyses that ILAS observed STS.

[20] Figure 2 also shows some discrepancies between the measurements and the theoretical prediction for STS. According to the thermodynamic model, the extinction data for the events from 1 to 8 should be much larger and nitric acid mixing ratio should be much lower than that observed. Several factors could have contributed to these discrepancies. The first possible factor is nonequilibrium particle formations under the influence of the mountain waves. Data numbered from 1 to 8 in the figures were obtained downwind from Scandinavia, and it is possible that the air mass observed has been influenced by lee waves. If that is indeed what happened, these STS droplets may not have attained equilibrium with the gas due to mesoscale cooling events, as discussed by Voigt *et al.* [2000], who concluded that nonequilibrium compositions are a dominant feature of STS near T_{ice} under the activity of gravity waves.

[21] The second possibility is the suppression of STS growth due to the coexistence of ice particles. Pan *et al.* [2002] analyzed ILAS water vapor data and found significant gas phase water vapor reduction and dehydration in mid-January associated with ice particle formation. The events that show large water vapor reduction include the PSC events shown in Figure 3. ILAS retrieval error analyses [Yokota *et al.*, 2002] indicate that, without the presence of NAT particles, the retrieved water vapor data are reliable even in the presence of ice PSCs. The spectral analyses of extinction data support the absence of NAT in the mid-January time period. These lead to the possibility that the STS growth was suppressed in dehydrated air. In fact, our sensitivity analyses show that if the water vapor used in the thermodynamic model calculation is ~ 1 ppmv lower, the STS theoretical lines shift leftward and the agreement between the observations and the STS theoretical lines for these events is improved.

[22] The third factor that could have contributed to the discrepancies is the inhomogeneity in the volume sampled by the satellite sensor. An occultation sensor like the ILAS has a relatively wide horizontal resolution along its line of sight, which is about 200 km at an altitude of 20 km. Its large sampling volume could make the characteristics of the observed data ambiguous, especially when a mixture of several compositions were observed. When spatial scale of a cloud is less than the sampling volume, we see only less volume enhancement and less decrease in nitric acid amount than expected from theory. Therefore, a mixture of STS and ice would be a reasonable interpretation to explain the synchronous decrease in nitric acid and water vapor.

[23] The last factor, but not the least, is the uncertainty in synoptic temperature data, such as UKMO data, which greatly complicates the comparison between the theoretical prediction and the observations. The magnitude of the bias and random error in synoptic temperature database varies with altitude, season, and geographical region, making it



(a)

(b)

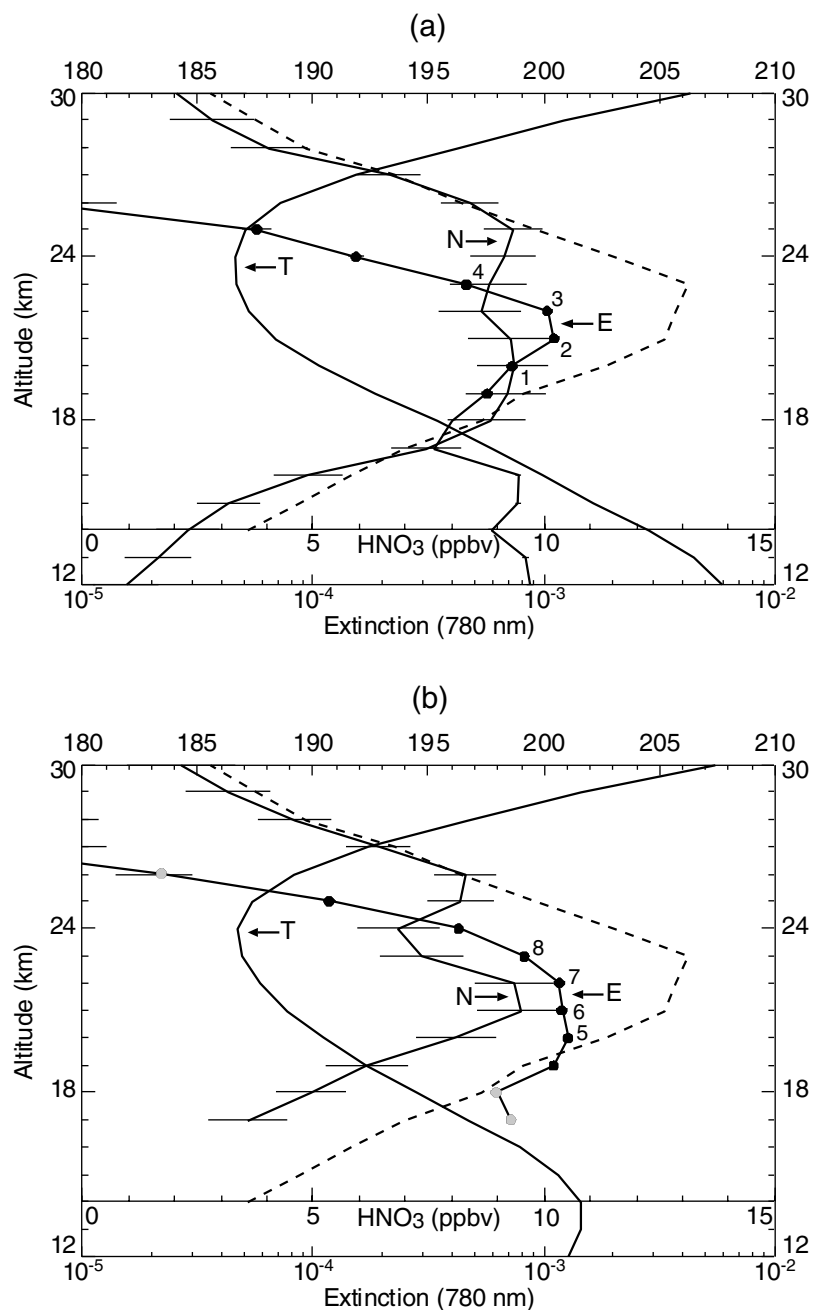


Figure 3. The vertical profiles of the extinction coefficient (E), nitric acid (N), and collocated UKMO temperature (T) observed on 19 January (65.8°N, 21.6°E) (a) and 20 (65.9°N, 28.9°E) (b). The 10-day averaged background profile of nitric acid for mid-January is also shown in the figure (dashed line). The black and gray circles represent data identified as PSCs. The black circles indicate the data that correspond to the STS formation curve.

Figure 2. (opposite) Scatterplots of UKMO temperature versus the ILAS extinction coefficient (a1–a4) and UKMO temperature versus the ILAS nitric acid (b1–b4) at 20–23 km in mid-January. Each panel represents a 1-km altitude level: (a1) extinction coefficient at 20 km, (a2) 21 km, (a3) 22 km, (a4) 23 km; (b1) mixing ratio of nitric acid at 20 km, (b2) 21 km, (b3) 22 km, (b4) 23 km. Error bars for the ILAS data are shown in the figure. Solid circles represent the data identified as PSCs. The red circles indicate the events consistent with the theoretical values of STS. Data numbered 1 to 4 come from the profile observed on 19 January and those numbered 5 to 8 from the profile observed on 20 January. The theoretical curves for STS (red lines), NAD (green line), and NAT (blue line) are shown in the figure. The thick solid red lines are based on the proper conversion factors depending on temperature. The thin dashed red lines are also shown for reference. See text about more details. Ice frost points (T_{ice}) are calculated using the total background amount of water vapor for each altitude level *Marti and Mauersberger* [1993].

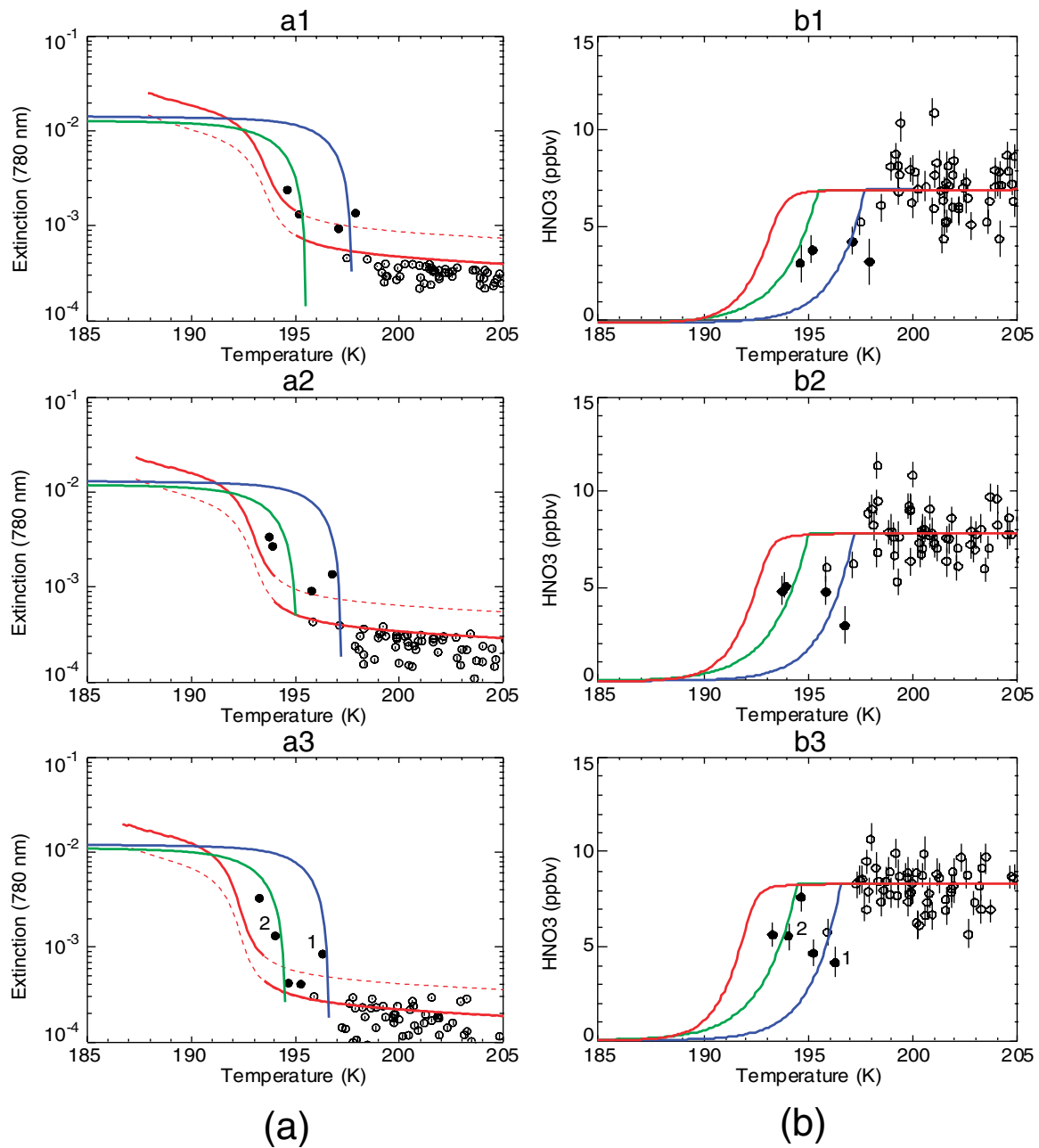


Figure 4. The same as Figure 2, but in early March, at 16–18 km: (a1) 16 km, (a2) 17 km, (a3) 18 km, (b1) 16 km, (b2) 17 km, (b3) 18 km.

difficult to estimate the uncertainty of individual collocated temperature data. Pullen and Jones [1997] reported the UKMO temperature has a 1.7 K positive bias and about 2 K of random scatter around T_{NAT} . Manney *et al.* [1996] derived much larger bias of 3.7 K for cold area ($T < 200$ K) in January. Pan *et al.* [2002] showed that ILAS water vapor data is consistent with a ~ 3.5 K warm bias in the UKMO data. Figures 2a1–2a4 also show ice frost points (T_{ice}) calculated using the total background amount of water vapor [Marti and Mauersberger, 1993]. If the temperature bias is as large as ~ 3 K, coexistence of ice would be possible. There are some other reports of even larger bias, depending meteorological conditions. Dörnbrack *et al.* [2001] presented significant warm bias in synoptic temper-

ature analysis under active mountain-induced lee waves over Scandinavia in January 1997.

3.4.2. Early March

[24] In 1997, break up of the polar vortex occurred later than usual, and it was reported that PSCs were observed by the ILAS until early March of that year near 120°E at relatively low altitudes [Hayashida *et al.*, 2000a, Plate 1c]. These were caused by the displacement of a cold air mass following the movement of the polar vortex. Figure 4 shows the scatterplots of the ILAS extinction coefficient and nitric acid data at 16–18 km in early March. Although a few PSCs were observed in March, both the extinction and nitric acid values suggest the existence of NAD or NAT. After comparison with the theoretical values, most of

Table 1. Summary of the Ratio of the Number of Classified Events in Each Category to the Total Number of PSC Events

	STS	NAD/NAT	Unclassified	All PSC Events
Jan.	32.4	23.6	44.0	148
Feb.	9.5	30.2	60.3	63
Mar.	3.2	64.5	32.3	31

All the PSC events were categorized into specific groups based on comparison of the ILAS extinction and nitric acid data with the theoretical predicted values. The ratios of the number of events for each category to the total number of PSC events in January, February, and March are indicated in the left three columns. The unit is percent (%). The total numbers of PSC events observed for each month are also shown in the rightmost column.

the events with enhanced extinction in the intense PSC layers late in the PSC season could be categorized into NAD or NAT (nitric-acid-containing solid PSCs).

[25] It is difficult to identify which composition is reliable for some data plotted between the red (STS curve) and green (NAD curve) lines, when considering the temperature uncertainty. For NAT cases, however, discrimination between STS and NAT could be easier, because the theoretical curves of NAT and STS are far enough apart.

[26] On the contrary to the STS events discussed above, the PSC events observed near 120°E, shown in Figure 4, have undergone relatively moderate temperature changes, which will be discussed in the next section. It implies an assumption of an equilibrium state would be reasonable, though there are many discussions on nonequilibrium transition during solid particle formation. At any rate, it is apparent that the scatterplots in Figure 4 have quite different feature from those in Figure 2.

[27] Table 1 summarizes the ratio of the number of classified events in each category to the total number of PSC events in January, February, and March. Many STS PSCs were observed at an earlier stage of the PSC season, while the observed NAD/NAT ratio became higher at a later stage. Some of the extinction coefficients and nitric acid values lying between the theoretically predicted values could not be categorized into any. Those events are shown as “unclassified” in Table 1.

4. Thermal History of PSC Particles

[28] The 20-day isentropic backward trajectory was calculated by using the European Centre for Medium-Range Weather Forecasts (ECMWF) TOGA Basic Level III temperature data to examine the thermal conditions at the synoptic scale for the observed PSC particles. The Earth Observation Research Center-Trajectory Analysis Model (EORC-TAM) developed by NASDA/EORC was used. See *Matuzono et al.* [1998] for details of this model. The backward trajectories were also calculated for four surrounding points, 100 km north, south, east, and west of the measurement point, to investigate the variability of conditions which may depend on small difference in location considering a rather large ILAS sampling volume. If the position and temperature histories of the measurement point and the four surrounding points diverged considerably over a few days, such trajectory clusters were excluded from the analysis, since they likely had a lot of uncertainties. Figure 5 illustrates typical temperature histories of the PSC events

that suggest the formation of STS as described in section 3. The thick black lines are the temperature histories from the ILAS measurement locations, and the bars show the range of divergence of the four surrounding points. In the temperature scale, the solid black, dashed black, solid gray, and dashed gray lines indicate the sulfuric acid tetrahydrate (SAT) melting temperature (T_{SAT}) [*Zhang et al.*, 1993], NAT saturation temperature (T_{NAT}) [*Hanson and Mauersberger*, 1988], SAT deliquescence temperature (T_{del}) [*Koop and Carslaw*, 1996], and ice frost point (T_{ice}) [*Marti and Mauersberger*, 1993], respectively. They are calculated using the background nitric acid and water vapor values determined for each 10-day period.

[29] The feature of the temperature history of STS events was rapid cooling just before the measurements. In more detail, they can be categorized into two different patterns, as indicated in Figures 5a and 5b. The air mass shown in Figure 5a experienced T_{SAT} one day before measurement, with a subsequent decrease in temperature until it was observed. At the time of observation, the temperature was still above T_{ice} ; therefore, the observed PSCs would have been liquid (STS), as far as warm bias in ECMWF temperature is about 1.4–1.6 K as reported by *Knudsen* [1996]. The temperature history in Figure 5b is that of PSC event numbered 2 in Figure 3a. Although the air mass shown in Figure 5b never experienced temperature exceeding T_{SAT} unlike the temperature history in Figure 5a, it almost always experienced temperatures above T_{NAT} until about two days before the observation, then fell below T_{NAT} , but never below T_{ice} . Therefore, liquid droplets (STS) would be most plausible as observed PSC type [*Tabazadeh et al.*, 1995].

[30] However, as already mentioned in the previous section, PSC event numbered 2 was observed downwind of the Scandinavia. The shaded area labeled “S” in Figure 5 indicates the time when air mass passed over the mountains of Scandinavia. As discussed above, the event seems to have been influenced by gravity waves, and possibility of ice formation should not be excluded if local cooling caused by mountain lee waves was significant.

[31] NAT and NAD PSCs were observed over a vertical range of several kilometers on 9 and 10 March, as shown in Figure 4. Figure 6 shows the temperature histories of these PSC events. The temperature history in Figure 6b is that of PSC event numbered 1 in Figures 4a3 and 4b3, and the history in Figure 6c is that numbered 2 in Figures 4a3 and 4b3. T_{SAT} , T_{NAT} , T_{del} , and T_{ice} are calculated using the background nitric acid and water vapor values determined for each 10-day period. The background nitric acid value of 9.2 ppbv based on the 10-day average of ILAS data at 20 km for early March is much lower than the background in mid-January (11.4 ppbv). The PSC events shown in Figure 6 clearly experienced temperatures below T_{NAT} for a longer period than those in Figure 5. They sometimes fell below T_{ice} during the 20-day period shown in the figure. *Larsen et al.* [1997] suggested that PSC particles might freeze if they experienced synoptic temperatures below T_{NAT} for at least 1–2 days, possibly accompanied by synoptic temperature fluctuations, and this supports the freezing scenario of *Tabazadeh et al.* [1995]. The nitric-acid-containing solid PSC events observed in early March experienced temperatures below T_{NAT} for more than several days, which is consistent with the study of *Larsen et al.* [1997].

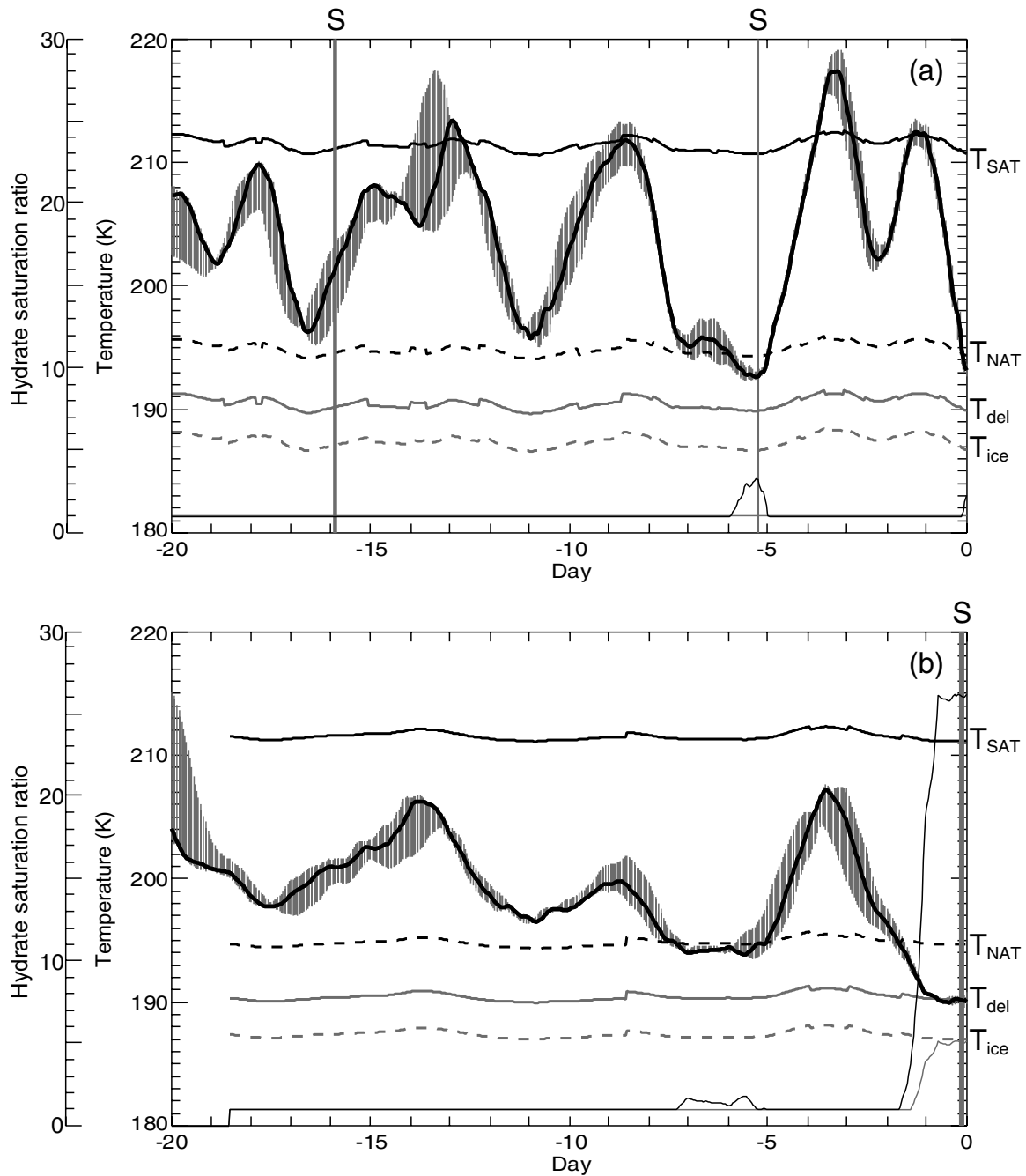


Figure 5. Typical temperature histories of PSC events suggesting the formation of STS PSCs: (a) at 22 km on 19 January, (b) at 21 km on 19 January. The thick black lines indicate the temperature histories from the ILS measurement locations. The bars show the range of divergence of the four surrounding points. In the temperature scale, the solid black, dashed black, solid gray, and dashed gray lines indicate the sulfuric acid tetrahydrate (SAT) melting temperature (T_{SAT}) Zhang *et al.* [1993], NAT saturation temperature (T_{NAT}) Hanson and Mauersberger [1988], SAT deliquescence temperature (T_{del}) Koop and Carslaw [1996], and ice frost point (T_{ice}) Marti and Mauersberger [1993], respectively. The 10-day background amounts of nitric acid and water vapor are used in the calculations. The shaded area labeled “S” indicates that the air mass passed over Scandinavian mountains. The NAT and NAD saturation ratios in solution calculated along with the trajectory using the 10-day background amounts of nitric acid and water vapor are depicted by thin black and gray lines, respectively.

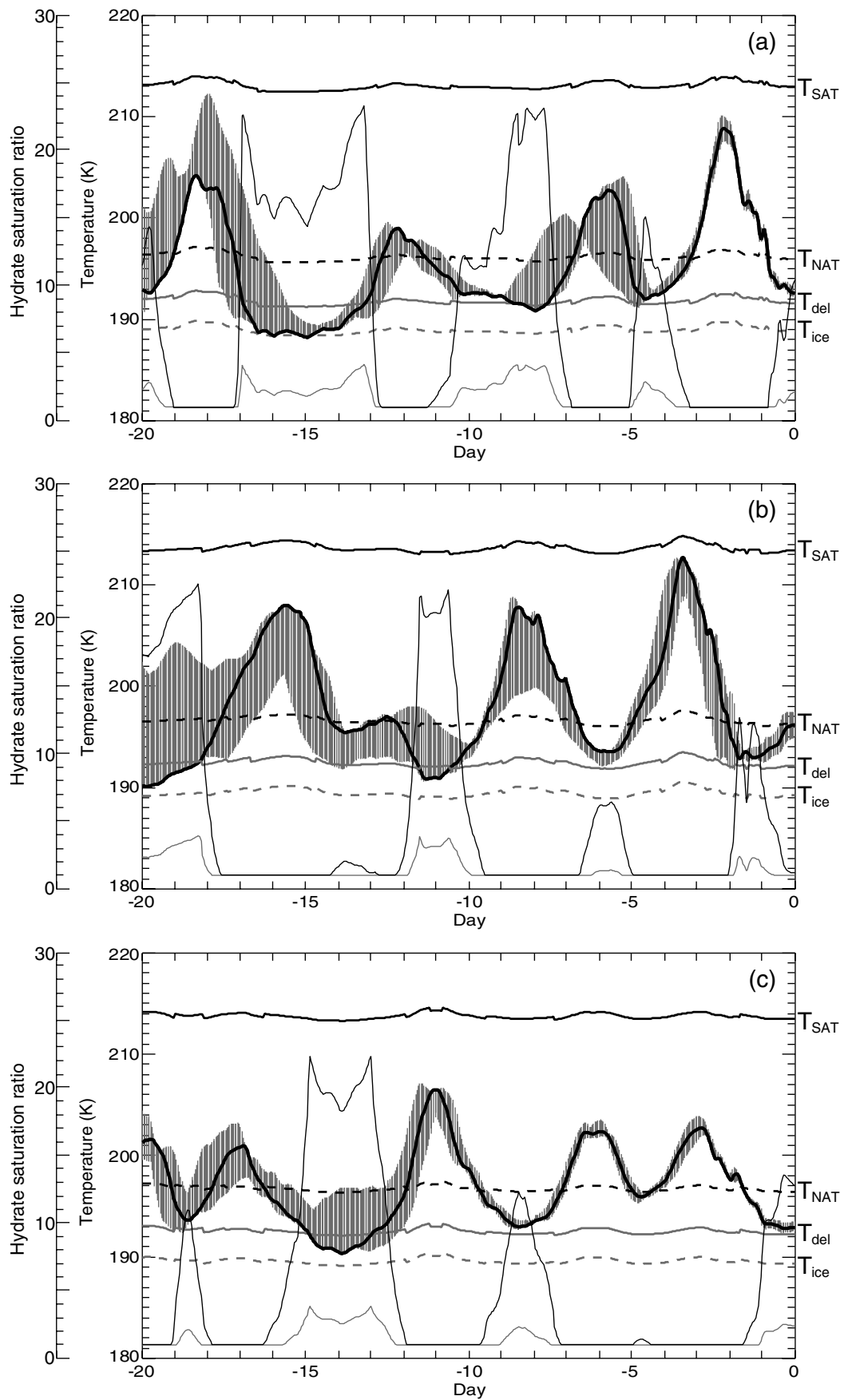


Figure 6. The same as Figure 5, but for nitric-acid-containing solid PSCs observed in early March: (a) at 19 km on 9 March, (b) at 18 km on 10 March, (c) at 18 km on 10 March.

[32] In contrast to the event in Figure 5b, all the events shown in Figure 6 were observed over Siberia ($\sim 120^\circ\text{E}$), not downwind of high mountainous areas. Therefore, they are unlikely to have been influenced by a mountain-induced lee wave. This suggests that their formation processes should be explained from their synoptic scale temperature histories.

[33] The hydrate saturation ratios of liquid were calculated along with the trajectory. The amounts of nitric acid, water vapor, and sulfate used in the calculations were the background values for each 10-day period. In Figures 5 and 6, the thin black and gray lines depict the NAT and NAD saturation ratios, respectively. The PSC events shown in Figure 6 maintained relatively high nitric acid hydrate saturation ratios for 20 days in contrast to those in Figure 5. A higher saturation ratio produces a higher homogeneous nucleation rate of nitric acid hydrates [Salcedo *et al.*, 2001], and therefore, these solid PSCs would freeze homogeneously [Salcedo *et al.*, 2001; Tabazadeh *et al.*, 2001].

[34] Although the homogeneous nucleation theory seems to explain the formation process of the observed solid particles, we cannot neglect the possibility of heterogeneous nucleation on SAT for those events. As shown in Figure 6, the air masses were exposed to temperatures below T_{NAT} for a long time, and sulfuric aerosols might have formed SAT. The temperature occasionally dropped to T_{del} , when ECMWF warm bias is into consideration. Under the usual stratospheric conditions, SAT deliquesces into ternary solution at T_{del} upon cooling. However, SAT does not completely deliquesce into ternary solution above T_{ice} in a denitrified air mass [Martin *et al.*, 1998]. Kondo *et al.* [2000] reported significant denitrification in an analysis of ILAS nitric acid data in February and March 1997. Therefore, in this case, SAT might have remained frozen until observed.

[35] Some PSC events with a significantly low nitric acid value were observed from mid-February to early March. Their decrease in nitric acid cannot be explained by any theoretical predictions. Close examination of the temperature histories of these PSC events makes it clear that they had experienced temperatures around T_{ice} or lower for a fairly long time before the measurements. Exposure to such low temperatures would generate large particles, leading to denitrification. The PSC events with low gaseous nitric acid might be observed as ongoing denitrification. Actually, the nitric acid values inside the polar vortex in March were smaller than in January, as mentioned above. Even if the temperature fell low enough to generate PSCs, particle growth would be limited by the insufficient amount of nitric acid, in such denitrified air masses. In this case, the extinction is not as high as expected from theory, with very low gaseous nitric acid.

5. Summary

[36] The ILAS successfully observed the profiles of aerosol extinction, nitric acid, and water vapor in both pole regions from November 1996 through June 1997. We identified about 250 events in 65 profiles as PSCs.

[37] This study compared the ILAS extinction and nitric acid data with theoretically predicted values assuming the existence of STS, NAD, and NAT. In mid-January, both the

extinction coefficient and nitric acid level of some of the observed PSC events showed better agreement with the theoretical values for STS than with those of NAT or NAD. They showed that the enhanced volume corresponds to the decrease in the ambient nitric acid, suggesting the uptake of nitric acid into particles as STS forms. The ILAS observed STS PSCs over a wide vertical range on 19 and 20 January. On the other hand, a corresponding decrease in water vapor was reported by Pan *et al.* [2002]. Mixture of STS and ice in a large sampling volume of ILAS would be a reasonable interpretation to explain the synchronous decrease in nitric acid and water vapor. It would be also possible that the particle growth was limited in dehydrated air. Although a few PSCs were observed in March, most of the characteristic PSC events in the late PSC season were categorized as NAD or NAT. The result of PSC classification was summarized in Table 1.

[38] The 20-day isentropic backward trajectory was calculated using ECMWF TOGA Basic Level III temperature data to examine the thermal conditions in synoptic scale for the observed PSC particles. The temperature histories of the STS events indicate that no sulfuric hydrate or ice particles suitable as nuclei for solid PSCs could have existed in the ambient air before the measurements, and therefore, liquid droplets (STS) could form. However, more detailed analysis of mesoscale cooling is needed to understand ice formation under the perturbed conditions by mountain-induced lee waves.

[39] The nitric-acid-containing solid PSC events observed in early March experienced temperatures below T_{NAT} for more than several days, and sometimes fell below T_{ice} during the 20-day period, which is consistent with the study by Larsen *et al.* [1997]. They had not passed over typical mountainous area before their measurements, so the formation mechanisms of these solid particles should be explained from their synoptic scale temperature histories, without considering lee waves. They maintained relatively high nitric acid hydrate saturation ratios along their trajectory, which suggests their homogeneous nucleation.

[40] From mid-February to early March, some PSC events with significantly low nitric acid values were observed; temperatures had been around T_{ice} or lower for a fairly long time before the measurements. In these likely denitrified air masses, the shortage of nitric acid would limit particle growth, even if the temperature did fall low enough to generate PSCs.

[41] **Acknowledgments.** We wish to express our sincere thanks to all of the ILAS science team members and their associates. We thank Sergey Oschepkov for the helpful discussion and information on PSC discrimination using the ILAS aerosol extinction data. We are also grateful to Richard Swinbank for supplying the UKMO stratospheric assimilation data. We also thank NASDA/EORC for providing the EORC-TAM trajectory software programs. We obtained the OPC data from the ILAS Correlative Measurements DataBase (ILAS-CMDB). The ILAS retrieval data processing was carried out at the ILAS Data Handling Facility (DHF) at NIES. Financial support was partly provided by NASDA.

References

- Borrmann, S., S. Solomon, J. E. Dye, D. Baumgardner, K. K. Kelly, and K. R. Chan, Heterogeneous reactions on stratospheric background aerosols, volcanic sulfuric acid droplets, and type I polar stratospheric clouds: Effects of temperature fluctuations and differences in particle phase, *J. Geophys. Res.*, *102*, 3639–3648, 1997.
- Browell, E. V., et al., Airborne lidar observations in the wintertime Arctic

- stratosphere: Polar stratospheric clouds, *Geophys. Res. Lett.*, *17*, 385–388, 1990.
- Carslaw, K. S., B. P. Luo, S. L. Clegg, T. Peter, P. Brimblecombe, and P. J. Crutzen, Stratospheric aerosol growth and HNO₃ gas phase depletion from coupled HNO₃ and water uptake by liquid particles, *Geophys. Res. Lett.*, *21*, 2479–2482, 1994.
- Carslaw, K. S., B. Luo, and T. Peter, An analytic expression for the composition of aqueous HNO₃-H₂SO₄ stratospheric aerosols including gas phase removal of HNO₃, *Geophys. Res. Lett.*, *22*, 1877–1880, 1995.
- Carslaw, K. S., M. Wirth, A. Tsias, B. P. Luo, A. Dornbrack, M. Leutbecher, H. Volkert, W. Renger, J. T. Bacmeister, and T. Peter, Particle microphysics and chemistry in remotely observed mountain polar stratospheric clouds, *J. Geophys. Res.*, *103*, 5785–5796, 1998.
- Carslaw, K. S., T. Peter, J. T. Bacmeister, and S. D. Eckermann, Widespread solid particle formation by mountain waves in the Arctic stratosphere, *J. Geophys. Res.*, *104*, 1827–1836, 1999.
- Deshler, T., B. Nardi, A. Adriani, F. Cairo, G. Hansen, F. Fierli, A. Hauchecorne, and L. Pulvirenti, Determining the index of refraction of polar stratospheric clouds above Andoya (69 N) by combining size-resolved concentration and optical scattering measurements, *J. Geophys. Res.*, *105*, 3943–3953, 2000.
- Dörnbrack, A., M. Leutbecher, J. Reichardt, A. Behrendt, K.-P. Müller, and G. Baumgarten, Relevance of mountain wave cooling for the formation of polar stratospheric clouds over Scandinavia: Mesoscale dynamics and observations for January 1997, *J. Geophys. Res.*, *106*, 1569–1581, 2001.
- Dye, J. E., D. Baumgardner, B. W. Gandrud, S. R. Kawa, K. K. Kelly, M. Loewenstein, G. V. Ferry, K. R. Chan, and B. L. Gary, Particle size distributions in Arctic polar stratospheric clouds, growth and freezing of sulfuric acid droplets, and implications for cloud formation, *J. Geophys. Res.*, *97*, 8015–8034, 1992.
- Fahey, D. W., et al., The detection of large HNO₃-containing particles in the winter Arctic stratosphere, *Science*, *291*, 1026–1031, 2001.
- Fromm, M. D., J. D. Lumpe, R. M. Bevilacqua, E. P. Shettle, J. Hornstein, S. T. Massie, and K. H. Fricke, Observations of Antarctic polar stratospheric clouds by POAM II: 1994–1996, *J. Geophys. Res.*, *102*, 23,659–23,672, 1997.
- Hanson, D., and K. Mauersberger, Laboratory studies of the nitric acid trihydrate: Implications for the south polar stratosphere, *Geophys. Res. Lett.*, *15*, 855–858, 1988.
- Hayashida, S., N. Saitoh, A. Kagawa, T. Yokota, M. Suzuki, H. Nakajima, and Y. Sasano, Arctic polar stratospheric clouds observed with the Improved Limb Atmospheric Spectrometer during winter 1996/1997, *J. Geophys. Res.*, *105*, 24,715–24,730, 2000a.
- Hayashida, S., N. Saitoh, M. Horikawa, Y. Amemiya, C. Brogniez, T. Deshler, and Y. Sasano, Stratospheric background aerosols and polar stratospheric clouds observed with satellite sensors — Inference of particle composition and sulfate amount, *Soc. Photo Opt. Instrum. Eng.*, *76–86*, 2000b.
- Hervig, M. E., K. S. Carslaw, T. Peter, T. Deshler, L. L. Gordley, G. Redaelli, U. Biermann, and J. M. R. III, Polar stratospheric clouds due to vapor enhancement: HALOE observations of the Antarctic vortex in 1993, *J. Geophys. Res.*, *102*, 28,185–28,193, 1997.
- Hofmann, D. J., and T. Deshler, Stratospheric cloud observations during formation of the antarctic ozone hole in 1989, *J. Geophys. Res.*, *96*, 2897–2912, 1991.
- Hofmann, D. J., and J. M. Rosen, Sulfuric acid droplet formation and growth in the stratosphere after the 1982 eruption of El Chichon, *Science*, *222*, 325–327, 1983.
- Irie, H., et al., Validation of NO₂ and HNO₃ measurements from the Improved Limb Atmospheric Spectrometer (ILAS) with the version 5.20 retrieval algorithm, *J. Geophys. Res.*, *10.1029/2001JD001304*, in press, 2002.
- Kanzawa, H., et al., Validation and data characteristics of water vapor profiles observed by the Improved Limb Atmospheric Spectrometer (ILAS) and processed with Version 5.20 algorithm, *J. Geophys. Res.*, *10.1029/2001JD000881*, in press, 2002.
- Knudsen, B. M., Accuracy of arctic stratospheric temperature analyses and the implications for the prediction of polar stratospheric clouds, *Geophys. Res. Lett.*, *23*, 3747–3750, 1996.
- Koike, M., et al., A comparison of Arctic HNO₃ profiles measured by the Improved Limb Atmospheric Spectrometer and balloon-borne sensors, *J. Geophys. Res.*, *105*, 6761–6771, 2000.
- Kondo, Y., H. Irie, M. Koike, and G. E. Bodeker, Denitrification and nitrification in the Arctic stratosphere during the winter of 1996–1997, *Geophys. Res. Lett.*, *27*, 337–340, 2000.
- Koop, T., and K. S. Carslaw, Melting of H₂SO₄·4H₂O particles upon cooling: Implications for polar stratospheric clouds, *Science*, *272*, 1638–1641, 1996.
- Larsen, N., B. M. Knudsen, J. M. Rosen, N. T. Kjøme, and E. Kyro, Balloonborne backscatter observations of type 1 PSC formation: Inference about physical state from trajectory analysis, *Geophys. Res. Lett.*, *23*, 1091–1094, 1996.
- Larsen, N., B. M. Knudsen, J. M. Rosen, N. T. Kjøme, R. Neuber, and E. Kyro, Temperature histories in liquid and solid polar stratospheric cloud formation, *J. Geophys. Res.*, *102*, 23,505–23,517, 1997.
- Luo, B., U. K. Krieger, and T. Peter, Densities and refractive indices of H₂SO₄/HNO₃/H₂O solutions to stratospheric temperatures, *Geophys. Res. Lett.*, *23*, 3707–3710, 1996.
- Manney, G. L., R. Swinbank, S. T. Massie, M. E. Gelman, A. J. Miller, R. Nagatani, A. O. Neill, and R. W. Zurek, Comparison of U. K. Meteorological Office and U. S. National Meteorological Center stratospheric analyses during northern and southern winter, *J. Geophys. Res.*, *101*, 10,311–10,334, 1996.
- Marti, J., and K. Mauersberger, A survey and new measurements of ice vapor pressure at temperatures between 170 and 250 K, *Geophys. Res. Lett.*, *20*, 363–366, 1993.
- Marti, J. J., and K. Mauersberger, Evidence for nitric acid pentahydrate formed under stratospheric conditions, *J. Phys. Chem.*, *98*, 6897–6899, 1994.
- Martin, S. T., D. Salcedo, L. T. Molina, and M. J. Molina, Deliquescence of sulfuric acid tetrahydrate following volcanic eruptions or denitrification, *Geophys. Res. Lett.*, *25*, 31–34, 1998.
- Massie, S. T., et al., Simultaneous observations of polar stratospheric clouds and HNO₃ over Scandinavia in January, 1992, *Geophys. Res. Lett.*, *24*, 595–598, 1997.
- Matuzono, T., T. Sano, and T. Ogawa, *Development of the Trajectory Analysis Model (EORC-TAM)*, pp. 55–68, NASDA/EORC, Tokyo, 1998.
- Mehrten, H., and J. Reichardt, Particle properties of a PSC observed on January 19, 1997 above Andoya and Esrange, in *4th European Symposium on Polar Stratospheric Ozone*, pp. 147–150, Schliersee, Germany, 1997.
- Nakajima, H., et al., Characteristics and performance of the Improved Limb Atmospheric Spectrometer (ILAS) in orbit, *J. Geophys. Res.*, *10.1029/2001JD000607*, in press, 2002.
- Pan, L. L., W. J. Randel, H. Nakajima, S. T. Massie, H. Kanzawa, Y. Sasano, T. Yokota, T. Sugita, S. Hayashida, and S. Oshchepkov, Satellite observation of dehydration in the Arctic polar stratosphere, *Geophys. Res. Lett.*, *29*(8), 10.1029/2001GL014147, 2002.
- Poole, L. R., and M. C. Pitts, Polar stratospheric cloud climatology based on Stratospheric Aerosol Measurement II observations from 1978 to 1989, *J. Geophys. Res.*, *99*, 13,083–13,089, 1994.
- Pullen, S., and R. L. Jones, Accuracy of temperatures from UKMO analyses of 1994/95 in the arctic winter stratosphere, *Geophys. Res. Lett.*, *24*, 845–848, 1997.
- Ravishankara, A. R., and D. R. Hanson, Differences in the reactivity of Type I polar stratospheric clouds depending on their phase, *J. Geophys. Res.*, *101*, 3885–3890, 1996.
- Riviere, E. D., et al., Role of lee waves in the formation of solid polar stratospheric clouds: Case studies from February 1997, *J. Geophys. Res.*, *105*, 6845–6853, 2000.
- Russell, P. B., et al., Global to microscale evolution of the Pinatubo volcanic aerosol derived from diverse measurements and analysis, *J. Geophys. Res.*, *101*, 18,745–18,763, 1996.
- Salcedo, D., L. T. Molina, and M. J. Molina, Homogeneous freezing of concentrated aqueous nitric acid solutions at polar stratospheric temperatures, *J. Phys. Chem.*, *105*, 1433–1439, 2001.
- Santee, M. L., A. Tabazadeh, G. L. Manney, R. J. Salawitch, L. Froidevaux, W. G. Read, and J. W. Waters, UARS Microwave Limb Sounder HNO₃ observations: Implications for Antarctic polar stratospheric clouds, *J. Geophys. Res.*, *103*, 13,285–13,313, 1998.
- Santee, M. L., A. Tabazadeh, G. L. Manney, M. D. Fromm, R. M. Bevilacqua, and E. J. Jensen, Inferring PSC composition in the Arctic from UARS MLS HNO₃ and POAM II aerosol extinction measurements, in *Quadrennial Ozone Symposium*, pp. 199–200, Sapporo, Japan, 2000.
- Sasano, Y., M. Suzuki, T. Yokota, and H. Kanzawa, Improved Limb Atmospheric Spectrometer (ILAS) for stratospheric ozone layer measurements by solar occultation technique, *Geophys. Res. Lett.*, *26*, 197–200, 1999.
- Solomon, S., Stratospheric ozone depletion: A review of concepts and history, *Rev. Geophys.*, *37*, 275–316, 1999.
- Steele, H. M., and P. Hamill, Effects of temperature and humidity on the growth and optical properties of sulphuric acid-water droplets in the stratosphere, *J. Aerosol Sci.*, *12*, 517–528, 1981.
- Suzuki, M., A. Matsuzaki, T. Ishigaki, N. Kimura, N. Araki, T. Yokota, and Y. Sasano, ILAS, the Improved Limb Atmospheric Spectrometer, on the Advanced Earth Observing Satellite, *IEICE Trans. Fundam. Electron. Commun. Comput. Sci.*, *E78-B*(12), 1560–1570, 1995.
- Tabazadeh, A., O. B. Toon, and P. Hamill, Freezing behavior of stratospheric sulfate aerosols inferred from trajectory studies, *Geophys. Res. Lett.*, *22*, 1725–1728, 1995.

- Tabazadeh, A., E. J. Jensen, O. B. Toon, K. Drdla, and M. R. Schoeberl, Pole of the stratosphere polar freezing belt in denitrification, *Science*, 291, 2591–2594, 2001.
- Tolbert, M. A., Sulfate aerosols and polar stratospheric cloud formation, *Science*, 264, 527–528, 1994.
- Tolbert, M. A., Polar clouds and sulfate aerosols, *Science*, 272, 1597, 1996.
- Toon, O. B., and M. A. Tolbert, Spectroscopic evidence against nitric acid trihydrate in polar stratospheric clouds, *Nature*, 375, 218–221, 1995.
- Toon, O. B., M. A. Tolbert, B. G. Koehler, A. M. Middlebrook, and J. Jordan, Infrared optical constants of H₂O ice, amorphous nitric acid solutions, and nitric acid hydrate, *J. Geophys. Res.*, 99, 25,631–25,654, 1994.
- Tsias, A., A. J. Prenni, K. S. Carslaw, T. P. Onasch, B. P. Luo, M. A. Tolbert, and T. Peter, Freezing of polar stratospheric clouds in orographically induced strong warming events, *Geophys. Res. Lett.*, 24, 2303–2306, 1997.
- Voigt, C., A. Tsias, A. Dombrack, S. Meilinger, B. Luo, J. Schreiner, N. Larsen, K. Mauersberger, and T. Peter, Non-equilibrium compositions of liquid polar stratospheric clouds in gravity waves, *Geophys. Res. Lett.*, 27, 3873–3876, 2000.
- Waibel, A. E., T. Peter, K. S. Carslaw, H. Oelhaf, G. Wetzell, P. J. Crutzen, U. Poschl, A. Tsias, E. Reimer, and H. Fischer, Arctic ozone loss due to denitrification, *Science*, 283, 1999.
- Worsnop, D. R., L. E. Fox, M. S. Zahniser, and S. C. Wofsy, Vapor pressures of solid hydrates of nitric acid: Implications for polar stratospheric clouds, *Science*, 259, 71–74, 1993.
- Yokota, T., H. Nakajima, T. Sugita, H. Tsubaki, Y. Itou, M. Kaji, M. Suzuki, H. Kanzawa, J. H. Park, and Y. Sasano, Improved Limb Atmospheric Spectrometer (ILAS) data retrieval algorithm for Version 5.20 gas profile products, *J. Geophys. Res.*, 10.1029/2001JD000628, in press, 2002.
- Zhang, R., P. J. Wooldridge, J. P. D. Abbatt, and M. J. Molina, Physical chemistry of the H₂SO₄/H₂O binary system at low temperatures: Stratospheric implications, *J. Phys. Chem.*, 97, 7351–7358, 1993.

S. Hayashida and N. Saitoh, Faculty of Science, Nara Women's University, Kita-uoya Nishi-machi, Nara 630-8506, Japan. (sachiko@ics.nara-wu.ac.jp; naoko@leo.ics.nara-wu.ac.jp)

L. L. Pan, Atmospheric Chemistry Division, National Center for Atmospheric Research, Boulder, CO 80307, USA. (liwen@acd.ucar.edu)

Y. Sasano, National Institute for Environmental Studies, Tsukuba, Ibaraki 305-0053, Japan. (sasano@nies.go.jp)